

Numerical Analysis of Picosecond Pulse Propagation in a Tensile-Strained Semiconductor Optical Amplifier with Parameter Extraction using Frequency Resolved Optical Gating

Michael J. Connelly (1), Aisling Clark (2) Prince M. Anandarajah (2) and Liam P. Barry (2)

1) Optical Communications Research Group, Dept. Electronic and Computer Engineering, University of Limerick, Limerick, Ireland, michael.connelly@ul.ie. 2) RINCE, School of Electronic Engineering, Dublin City University, Dublin 9, Ireland, liam.barry@dcu.ie.

Abstract: A numerical model of picosecond pulse propagation in a tensile-strained bulk semiconductor optical amplifier is described. The phenomenological parameters were obtained using the Levenberg-Marquardt algorithm and experimental pulse amplitude and phase measurements obtained using frequency resolved optical gating.

Introduction

Semiconductor Optical Amplifiers (SOAs) have attracted much interest in applications in all-optical signal processing such as clock recovery and optical time division demultiplexing (OTDM). In such applications SOAs are used to amplify high-energy optical pulses with pulse widths of the order of picoseconds. Common optical pulse sources used in ultrafast optical communications include mode-locked lasers, gain-switched lasers, and CW lasers followed by electro-absorption modulators. These sources can all generate high quality pulses that exhibit low chirp and jitter and high temporal and spectral purity. Commercial picosecond mode-locked lasers are now available that are suitable for use in OTDM systems. It is of interest to model the propagation of such pulses through an SOA. Models can give greater insight into the physical processes occurring within SOAs and can also be used to design subsystems utilizing SOAs as active gain elements. Most pulse propagation models use a variant of a modified non-linear Schrödinger equation (MSE) that includes the SOA non-linearities that are relevant to the pulse time scale [1]. Pulse propagation through an SOA is strongly dependent on the SOA pulse shape. Both the pulse intensity and phase must be considered. The MSE includes a number of phenomenological parameters, whose magnitude determines the influence the corresponding physical effect has on pulse propagation. The principle physical effects that influence pulse distortion in the 2 ps regime are non-linear gain saturation, carrier heating, due to the combined effects of stimulated emission, free-carrier absorption and two-photon absorption (TPA). The phenomenological parameters must be obtained by a comparison between model predictions and experiment. The SOA modelled in this paper is a commercially available device manufactured by Kamelian. It has a tensile strained InGaAsP active region sandwiched between two InGaAsP separate-confinement heterostructure layers and operates in the 1.55 μm region. The device structure consists of central active

region waveguide of width 1.1 μm , thickness 0.1 μm and length 840 μm . The active region narrows linearly as a lateral taper of length 80 μm to width 0.5 μm at each end. The tensile strain is used to compensate for the different TE and TM confinement factors in order to achieve polarization independent operation. In this paper we model the propagation of 2 ps mode-locked laser pulses using the MSE through this type of SOA. In the model, the spatial dependency of parameters such as the saturation energy is included. The MSE phenomenological parameters are obtained using the Levenberg-Marquardt technique and experimental measurements of the amplifier pulse amplitude and phase using the technique of Frequency Resolved Optical Gating (FROG). FROG can be used to overcome the limitations of traditional methods of pulse characterisation and provides complete characterization in the spectral and temporal domains with corresponding phase information.

Pulse propagation model

The MSE used to model the propagation in the SOA of an optical field with complex amplitude $V(z, \tau)$ is given by [1],

$$\left[\frac{\partial}{\partial z} + \frac{\gamma(\tau)}{2} + \left(\frac{\gamma_{2p}}{2} + ib_2 \right) V(z, \tau)^2 \right] V(z, \tau) = \left\{ \frac{1}{2} g_N(z, \tau) [1 + i\alpha_N(z, \tau)] + \frac{1}{2} \Delta g_T(z, \tau) [1 + i\alpha_T(z, \tau)] - \frac{i}{2} \frac{\Gamma \partial g_m(z, \tau)}{\partial \omega} \Big|_{\omega_0} \frac{\partial}{\partial \tau} - \frac{1}{4} \frac{\Gamma \partial^2 g_m(z, \tau)}{\partial^2 \omega} \Big|_{\omega_0} \frac{\partial^2}{\partial \tau^2} \right\} V(z, \tau)$$

where the local time $\tau = t - z/v_g$ (z is the propagation direction) and v_g is the group velocity. In the model we also take into account the spatial and time dependency of the attenuation coefficient $\gamma(\tau)$ and linewidth enhancement factors $\alpha_N(\tau)$ (due to carrier density changes) and $\alpha_T(\tau)$ (due to carrier heating). γ_2 is the TPA coefficient. b_2 represents self-phase modulation. The change in the dynamic gain due to carrier heating is given by

$$\Delta g_T(z, \tau) = - \int_{-\infty}^{\infty} U(s) e^{-s/\tau_{ch}} \left[\begin{array}{l} h_1 |V(\tau - s)|^2 \\ + h_2 |V(\tau - s)|^4 \end{array} \right] ds$$

where h_1 is a phenomenological constant representing the contribution of SE and FCA to carrier heating and h_2 represents the contribution of TPA. $U(s)$ is the unit step function. The dynamic gain due to carrier density changes is given by

$$g_N(z, \tau) = \Gamma g_m(z) \exp \left[- \frac{1}{W_s(z)} \int_{-\infty}^{\tau} e^{-s/\tau_s} |V(s)|^2 ds \right]$$

where $g_m(z)$, $W_s(z)$ and τ_s are the unsaturated material gain coefficient, saturation energy and spontaneous lifetime respectively. $g_m(z)$ is determined, for a given bias current, using the steady-state model [2]. $W_s(z)$ is a function of z due to the spatial dependency of the optical confinement factor. Both g_m and W_s are also polarisation dependent and are shown in Fig. 1. The derivatives $\partial g_m(\tau, \omega) / \partial \omega|_{\omega_0}$ and $\partial^2 g_m(\tau, \omega) / \partial \omega^2|_{\omega_0}$ and

the linewidth enhancement factors can also be determined from the steady-state model and are shown in Fig. 2 and Fig. 3 as a function of g_m .

Numerical solution and experiment

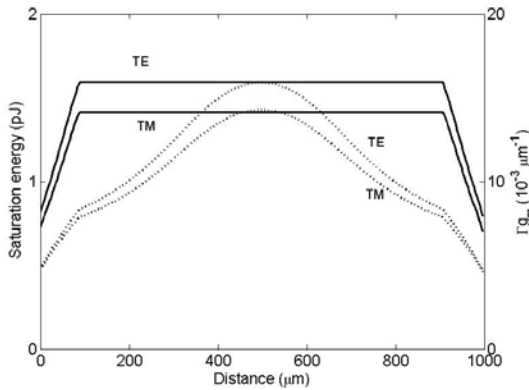


Fig. 1: Unsaturated TM polarisation dependent saturation energy (solid line) and material gain coefficient spatial distributions for a bias current of 200 mA, which corresponds to a fibre-to-fibre gain of 24 dB.

The MSE can be solved by using the finite-difference beam propagation method described in [3]. However in order to obtain good agreement between model predictions and experiment the phenomenological constants must be known. In this work we are particularly interested in the dynamics of the propagation of 2 ps mode-locked laser pulses. To determine the phenomenological constants, we first characterised the amplitude and phase of a 10 GHz repetition

rate 2 ps pulsewidth commercial mode-locked laser. The pulses were then amplified and the amplified pulse stream also characterised using FROG [4]. It is well known that the distortion experienced by pulses amplified by an SOA is very sensitive to the input pulse shape. In this work we use the experimentally measured complex pulse amplitude as the model input. In order to determine the phenomenological constants h_1 , h_2 , γ_{2p} and τ_{ch} we use the pulse propagation model and the Levenberg-Marquardt technique to determine the values of the parameters that minimise the r.m.s. error between the normalised predicted and experimental amplified pulse power for

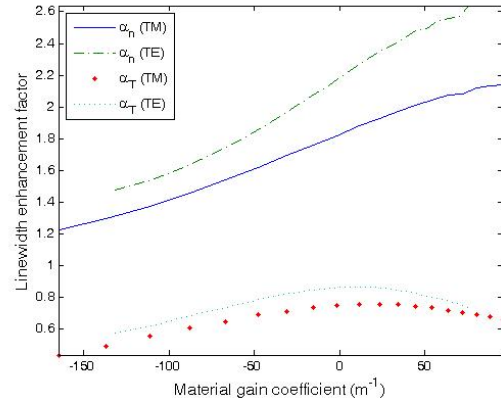


Fig. 2: Polarisation dependent linewidth enhancement factors versus corresponding polarisation dependent material gain coefficient.

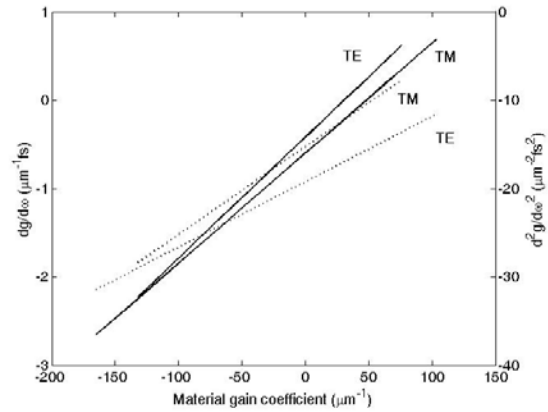


Fig. 3: First (solid line) and second order gain dispersion versus material gain.

three different input pulse peak powers ranging from low to high saturation. Once these values have been obtained, we then adjust the value of h_2 in order to obtain a reasonable match between the predicted and experimental frequency chirp of the amplified pulses. The normalised predicted and experimental input and amplified pulse power is shown in Fig. 4. The predicted and experimental pulse chirp is shown in Fig. 5. The agreement between experiment and the numerical model using the extracted parameters is good for the pulse power temporal profile. In the case of

the pulse chirp, although the magnitude of the predicted chirp and its slope is similar to the experimental results, the agreement is not as good. This is because the temporal distortions of the pulse power in the 2 ps regime are primarily due to the effects of the

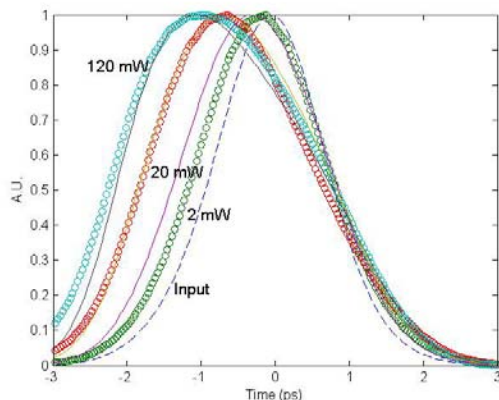


Fig. 4: Experimental ('o') and predicted (solid line) amplified pulse powers for TM polarisation at 1550 nm. The bias current is 200 mA and the parameter is the input pulse peak power.

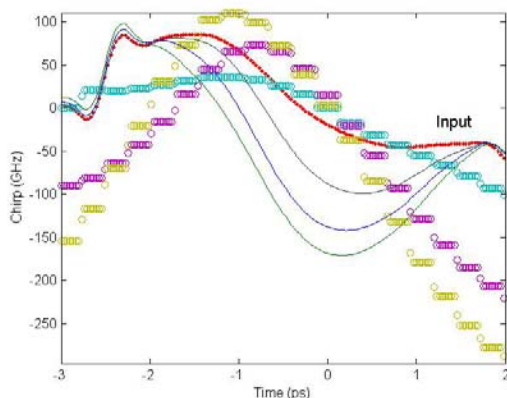


Fig. 5: Experimental ('o') and predicted (solid line) amplified pulse chirp for TM polarisation at 1550 nm for the pulses in Fig. 4. The chirp increases as the input power increases.

two types of gain saturation and the direct effect of TPA (i.e. the γ_2 term). However the phase evolution, and hence the chirp dynamics, is a result of a complicated addition of three types of self phase modulation, which are controlled by the changing pulse shape. It is also modified by the gain curvature and slope, which also depend on the pulse shape.

Conclusions

A numerical model for picosecond pulse propagation in tensile-strained SOAs has been developed. The phenomenological model parameters representing the various non-linear processes in the SOA are determined using a parameter extraction algorithm and experimental FROG measurements of amplified mode-locked laser pulses. There is good agreement between experiment and model predictions of the amplified pulse temporal power. However the ampli-

fied pulse chirp is more difficult to predict due to the complexity of the self-phase modulation processes in the SOA, and possibly requires the development of a more accurate propagation model.

Acknowledgments

This work was supported by Science Foundation Ireland Investigator Grant 02/IN1/I42. The author thanks A.E. Kelly of Amphotonix Ltd. for supplying the Kamelian SOA parameters and useful discussions.

References

- 1 M.Y. Hong et. al, IEEE J. Quantum Electron., no. 4, pp. 1122, 1994.
- 2 M.J. Connelly, IEEE J. Quantum Electron., no. 1, pp. 47, 2007.
- 3 N.K. Das, et al. IEEE J. Quantum Electron., no. 10, pp. 1184, 2000.
- 4 A.M Clarke et. al. IEEE Photon Tech. Lett., no. 9, pp. 1800, 2005.